

Deep Levels and Radiation Effects in p-InP

W.A. Anderson, A. Singh, K. Jiao and B. Lee
Center for Electronic and Electro-optic Materials
State University of New York at Buffalo
Electrical and Computer Engineering
Room 217C Bonner Hall
Amherst, NY 14260

Summary

A survey was conducted on past studies of hole traps in InP. An experiment was designed to evaluate hole traps in Zn-doped InP after fabrication, after electron irradiation and after annealing using deep level transient spectroscopy. Data similar to that of Yamaguchi was seen with observation of both radiation-induced hole and electron traps at $E_A = 0.45$ eV and 0.03 eV, respectively. Both traps are altered by annealing. It is also shown that trap parameters for surface-barrier devices are influenced by many factors such as bias voltage, which probes traps at different depths below the surface. These devices require great care in data evaluation.

Introduction

InP is an important material for the fabrication of solar cells for space applications [refs. 1-4] because of the high conversion efficiency and radiation resistance. Applications as detectors, high-speed transistors and quantum well structures also benefit from radiation hardness and high carrier mobility. Deep levels in the material can play an important role in limiting the minority carrier lifetime and therefore controlling the performance in electro-optic applications. A search of the literature reveals very few reports on the study of deep level traps in p-InP.

Bremond [ref. 5] studied bulk p-type InP using DLTS to reveal hole traps with $E_A=0.36$ and 0.70 eV. Sibille [ref. 6] examined Ti-Au Schottky diodes on (100) Zn-doped LPE layers to reveal a hole trap with $E_A=0.14$ eV. More recently, Yamaguchi [ref. 7] has studied effects of 1.0 MeV electron irradiation of n^+-p (Zn-doped) InP to reveal radiation-induced traps with $E_A=0.37$ and 0.52 eV, in agreement with Sibille [ref. 6]. It is the purpose of this paper to present a thorough study of both hole and electron traps in the same p-InP substrate, using a very high Schottky barrier to the p-InP provided by Yb metal. We have used the standard boxcar based DLTS technique [ref. 8] to determine the activation energy, capture cross section and concentration of the deep level traps. In addition, surface effects are separated from bulk effects in surface-barrier devices. These data may be useful to those using Zn-doped InP in device fabrication.

Experimental Method

Fabrication

Zn-doped p-InP, (100) orientation, one side polished, single crystal substrates used in this work were obtained from Crysta Comm. Inc. Before ohmic contact deposition, the substrates were ultrasonically rinsed in electronic grade trichloroethylene, acetone, methanol and deionized (DI) water. The samples were then etched for 30 s in $\text{H}_2\text{SO}_4 : \text{H}_2\text{O}_2 : \text{H}_2\text{O}$ (3:1:1) and $\text{HF} : \text{H}_2\text{O}$ (1:1) followed by DI water rinse and drying with gaseous N_2 . Au/Zn ohmic contacts were deposited at a pressure of 10^{-6} Torr and annealed in forming gas for 7 min. at 400°C . The polished surface was then etched in the above acid- H_2O rinse combination, protecting the back ohmic contact by a photoresist technique. Thermal oxide was grown for 45 min. at 350°C in 3 LPM gaseous O_2 . The resulting oxide thickness, measured with a Gaertner L117 ellipsometer was 20–35 Å. High barrier Schottky diodes were prepared by evaporating Yb dots of area $2.0 \times 10^{-2} \text{cm}^2$ onto the polished surface of p-InP. An illustration is given in Figure 1.

Measurements

DLTS measurements were performed by a computer controlled Bio-Rad Polaron S4600 DLTS system. The Yb/p-InP diodes were placed in a continuous flow liquid nitrogen cryostat which was typically cycled between 80 K and 450 K. A three terminal temperature controller, with microprocessor, controlled the temperature ramp programmer. A 1-MHz Boonton 72B capacitance meter with fast response time and a boxcar system with three sampling gates permitted the simultaneous measurement of DLTS spectra at two rate windows. Only the absolute value of the DLTS signal was plotted and the contributions due to the majority and the minority carriers represented as solid and dotted curves, respectively. The timing events were programmed so that for all the rate windows, the DLTS peak height, ΔC is one third of the true transient amplitude, ΔC_{TOT} . However, a gain of three is included so that ΔC_{TOT} equals the amplitude of the S4600 output at the DLTS peak. This feature facilitates the determination of trap concentrations.

The quiescent reverse bias applied to the Schottky diodes ranged between 0 V and 3 V. The forward filling pulse voltage was between 0 V and 0.6 V in the forward direction, with pulse widths between 1 μs and 50 ms. The temperature was swept at a rate of 0.2 K/s and the measurements performed for various rate windows between 20 s^{-1} and 10^3 s^{-1} . In order to investigate the interfacial traps, the quiescent voltage was set at a small forward bias (0.2 V) followed by a fill pulse of 0.6 V in the forward direction. The data acquisition system was controlled by an HP 9000 series computer. The capacitance transients were digitized, stored and analyzed by software to obtain trap parameters.

Irradiation and Annealing

After an initial DLTS study, samples were removed from the DLTS system and irradiated with the Au-leads intact. A 1.0 MeV van de Graaff generator was utilized with the samples resting on a water-cooled metal block. Samples were simultaneously irradiated to a fluence of $1 \times 10^{15} \text{e}^-/\text{cm}^2$ with great care to avoid heating during irradiation.

Samples were replaced in the DLTS system and re-tested prior to in situ annealing. Annealing was conducted in several stages with testing between each stage. The stages consisted of 200 mA/cm² for 15 min. at 300°K , 200 mA/cm² for 15 min. at 400°K , 100 mW/cm² illumination for 10 min.

at 300° K and 100 mW/cm² illumination for 10 min. at 400°K. These levels of injection and illumination are similar to those used by Yamaguchi et al [ref. 7].

Experimental Data

A typical DLTS scan for a Yb-MS device 44, given in Figure 2, reveals a majority (hole) trap and minority (electron) trap with activation energies (E_A) of 0.48 eV and 0.13 eV, respectively. After each preliminary scan, a C-V plot was conducted at the temperature of a particular DLTS peak. A more complete DLTS scan was then conducted to separately analyze each peak with six rate windows as illustrated in Figure 3 for the main peak before irradiation. The computer software then calculated trap parameters and gave an activation energy plot illustrated in Figure 4. Subsequent irradiation added a new hole with $E_A=0.45$ eV while slightly shifting the two original traps. This is illustrated by the DLTS scan of Figure 5.

Annealing procedures, outlined in the previous section, did not dramatically change the DLTS profile but did alter trap parameters as illustrated in Table 1. Radiation caused a slight shift and increased density of h1, the addition of a new hole trap (h2) and an energy shift plus change in capture cross-section of e1. Completion of annealing resulted in little change in h1, a significant decrease in σ for h2 with a downward shift in E_A , and little change in e1.

Discussion

A DLTS study was conducted for a Yb-MS device with data taken as fabricated, after irradiation and after annealing. Irradiation caused a new trap at $E_A = 0.45$ eV which shifted to 0.35 eV after annealing. Annealing caused a significant decrease in capture cross-section as well. Yamaguchi [ref. 7] observed radiation-induced traps H4 at $E_v + 0.37$ eV and E_2 at $E_c - 0.19$ eV which quite likely correspond to our h2 and e1 after irradiation. We did not observe the large annealing effect which he observed which may be related to irradiations at $1 \times 10^{16} \text{ e}^-/\text{cm}^2$ compared to our $1 \times 10^{15} \text{ e}^-/\text{cm}^2$.

A similar study performed on a Yb-MIS structure gave similar results although more noticeable changes were observed with annealing. Irradiation reduced the trap density and shifted E_A for the main hole trap and introduced a new electron trap at $E_A = 117$ meV. The altered hole trap is a combination of the original and a new one which could not be resolved. Annealing at 200 mA/cm² reduced the hole trap density but not the electron trap density. Optical annealing shifted electron traps and hole traps to a lower E_A , caused a shrinkage in the radiation-induced hole trap density and a growth of the original hole trap. These observations are similar to those of Yamaguchi [ref. 7] and are illustrated by Figure 6.

The difference in trap location between this work and that of Yamaguchi may be explained by a very thorough study by Singh [ref. 9]. It is evident that surface barrier devices provide different trap parameters with distance beneath the surface until the "true" bulk is reached. Thus, DLTS data on surface-barriers are influenced by surface preparation, type of metal, presence of an oxide, and bias levels used during measurement. This is illustrated by data of Table 2 which shows variation of parameters of a single trap with changes in reverse bias. The picture would be further complicated by effects of radiation and annealing which may contribute to variation in depletion width.

A further illustration is given in Table 3 as a report of hole traps in InP by other workers. Some differences are evident depending on type of device and method of semiconductor growth. These

differences are not nearly as severe as for electron traps in InP where almost every activation energy has been observed.

Conclusions

Data reported herein reveal trap introduction in p-InP due to e^- irradiation with subsequent changes upon annealing with forward bias and illumination. Annealing by current injection or photo-injection gives a different annealing behavior. Trap parameters are very sensitive to many conditions for surface barrier devices which requires great care in design of experiments and interpretation of data.

References

- [1] G.W. Turner, J.C.C. Fan and J.J. Hsich, Appl. Phys. Lett., **37**, 400 (1980).
- [2] A. Yamamoto, M. Yamaguchi and C. Vemura, Appl. Phys. Lett., **44**, 611 (1984).
- [3] A. Yamamoto, M. Yamaguchi and C. Vemura, Appl. Phys. Lett., **47**, 975 (1985).
- [4] T.J. Coutts and S. Naseem, Appl. Phys. Lett., **46**, 164 (1985).
- [5] D. Bremond, A. Nouailhat and G. Guillot, *Int. Symp. GaAs & Related Compounds*, Japan, 1981.
- [6] A. Sibille and J.C. Bourgoin, Appl. Phys. Lett., **41**, 956 (1982).
- [7] M. Yamaguchi, K. Ando, A. Yamamoto and C. Vemura, J. Appl. Phys., **58**, 568 (1985). ALSO Appl. Phys. Lett., **47**, 846 (1985).
- [8] D.V. Lang, J. Appl. Phys., **45**, 3023 (1974).
- [9] A. Singh and W.A. Anderson, submitted for publication.

TABLE 1.- TRAP DATA WITH IRRADIATION AND ANNEALING AS PARAMETERS

Sample	Activation Energy E_A (eV)	Capture Cross-Section σ (cm ²)	Trap Density N_T (#/cm ³)
44-h1	0.48	1.3×10^{-18}	3.5×10^{14}
44R-h1	0.50	2.6×10^{-18}	2.0×10^{15}
44RA-h1	0.50	3.5×10^{-18}	1.8×10^{15}
44R-h2	0.45	1.0×10^{-16}	2.0×10^{14}
44RA-h2	0.35	2.7×10^{-18}	3.5×10^{14}
44-e1	0.13	9.0×10^{-20}	4.0×10^{14}
44R-e1	0.031	1.1×10^{-21}	3.5×10^{14}
44RA-e1	0.038	8.0×10^{-22}	3.5×10^{14}

* R - irradiated

RA - annealed after irradiation

TABLE 2.- VARIATION OF THE PARAMETERS OF DOMINANT HOLE TRAP WITH QUIESCENT REVERSE BIAS IN Zn-DOPED p-InP BY DLTS USING SCHOTTKY DIODES [9]

Reverse Bias (V)	$E_{Tp} - E_V$ (eV)	σ_p (10^{-21} cm ²)	N_{Tp}^a (10^{14} cm ⁻³)	W^a (μ m)
3.0	0.56	4000	1.5	1.02
2.0	0.48	400	2.1	0.85
1.0	0.38	30	2.4	0.67
0.3	0.34	9	2.7	0.53
0.0	0.36	40	2.3	0.45
0.2 ^b	0.25	4	0.9	0.33

a. Space charge layer width.

b. Quiescent forward bias value.

TABLE 3.- PREVIOUS WORK ON HOLE TRAPS IN InP

<u>Identity</u>	<u>E_A</u>	<u>σ_2 (cm²)</u>	<u>N_T cm⁻³</u>	<u>REF*</u>	<u>Reason</u>
IH1	0.70			Bremond (81)	bulk p:Fe
H5	0.535	6E-15		Sibille (82)	LPE, Zn-doped, rad
H5	0.52			Yamaguchi (85)	<u>Zn-doped, rad.</u> point defect- impurity complex
IH2	0.48	1E-13		Bremond (81)	bulk p-undoped
H4	0.37	1.7E-15		Sibille (82)	LPE, Zn-doped, rad
H4	0.37	5E-15		Yamaguchi (85)	<u>Zn-doped, rad.</u> a recomb. center point defect
IH3	0.36			Bremond (81)	bulk p-undoped
H3	0.33	2.4E-15		Sibille (82)	LPE, Zn-doped, rad
H0	\approx 0.14			Sibille (82)	LPE,

* Bremond (81): LEC or VPE (n&p), Au-Schottky

Sibille (82): LPE on p⁺, <100> Zn-doped, 2E16, Ti-Au Schottky

Yamaguchi (84): n⁺/p(Zn) and p⁺/n(Si) [also seen as a minority trap in n-InP after irradiation]

Yamaguchi (85): n⁺/p diffused, Zn-doped (4.5E15-1E18)

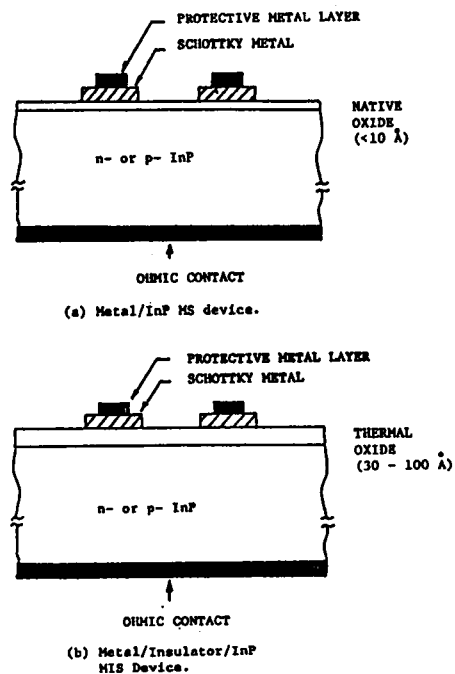


Figure 1 Diagram of samples studied by DLTS.

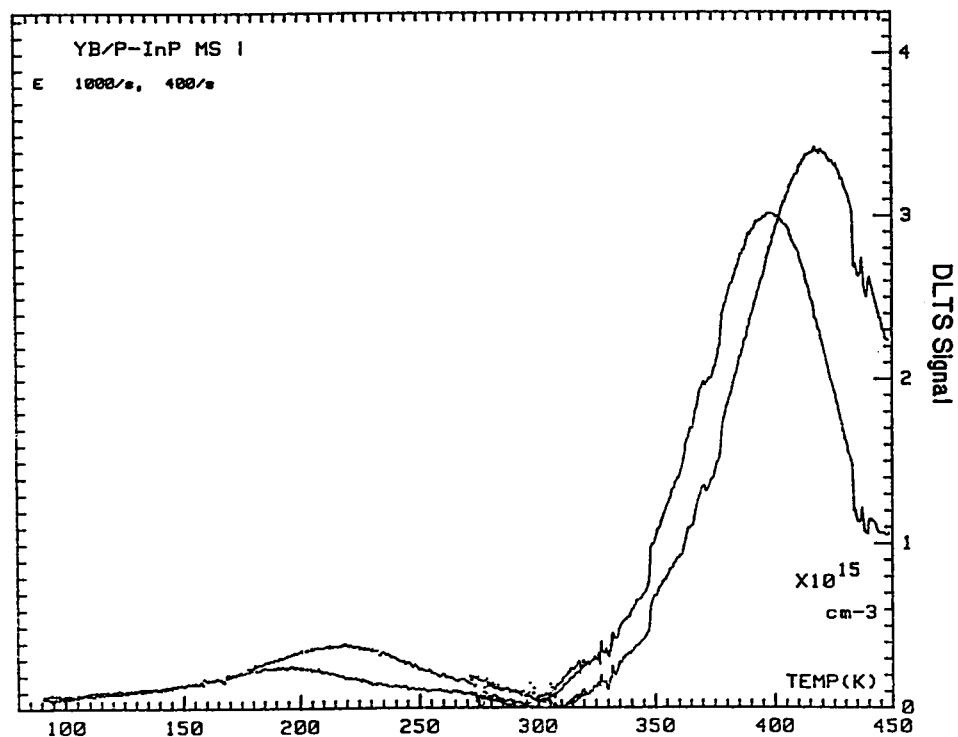


Figure 2 DLTS scan showing peak location prior to irradiation.

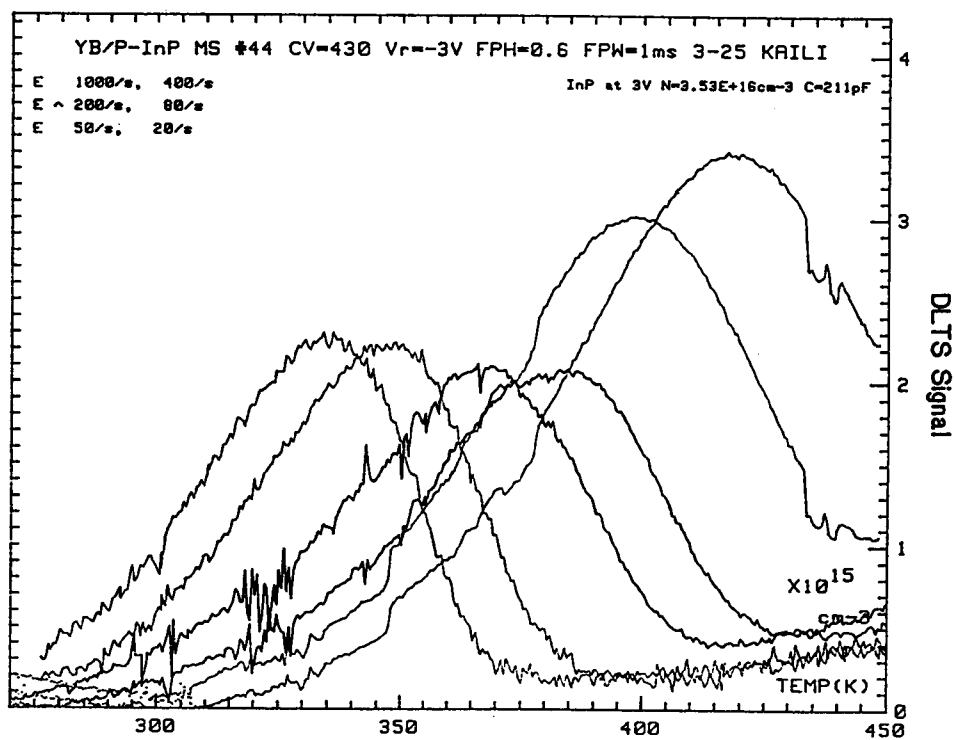


Figure 3 A complete DLTS analysis of the main hole trap prior to irradiation.

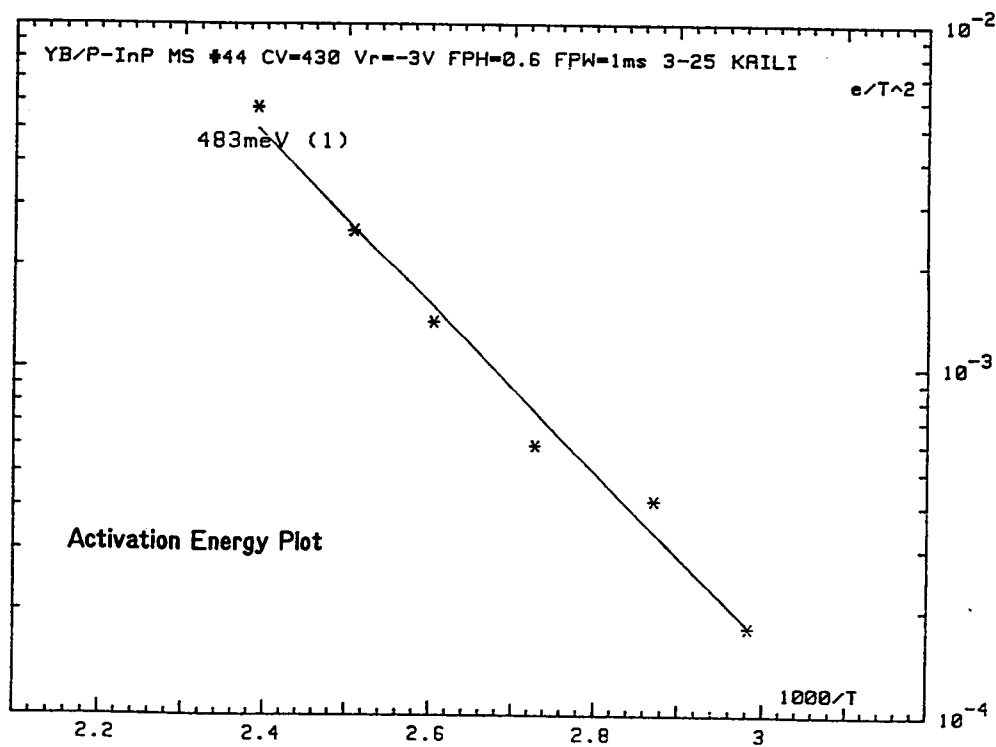


Figure 4 An activation energy plot prior to irradiation.

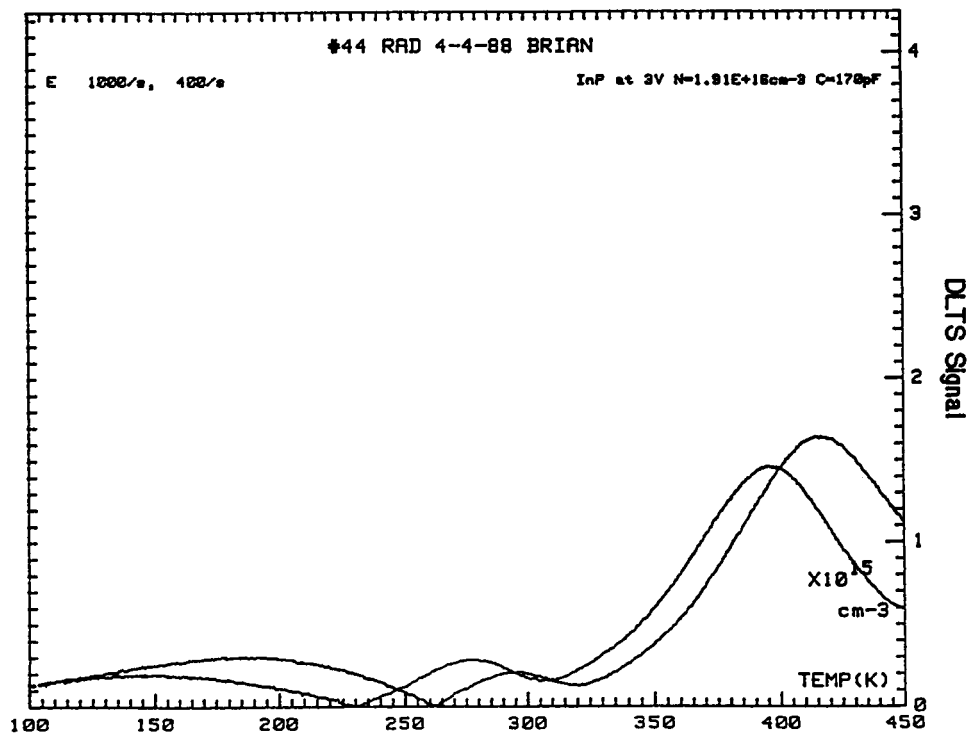


Figure 5 DLTS scan showing an added hole trap due to 1.0 MeV electron irradiation to a fluence of $1.0 \times 10^{15} \text{cm}^{-2}$.

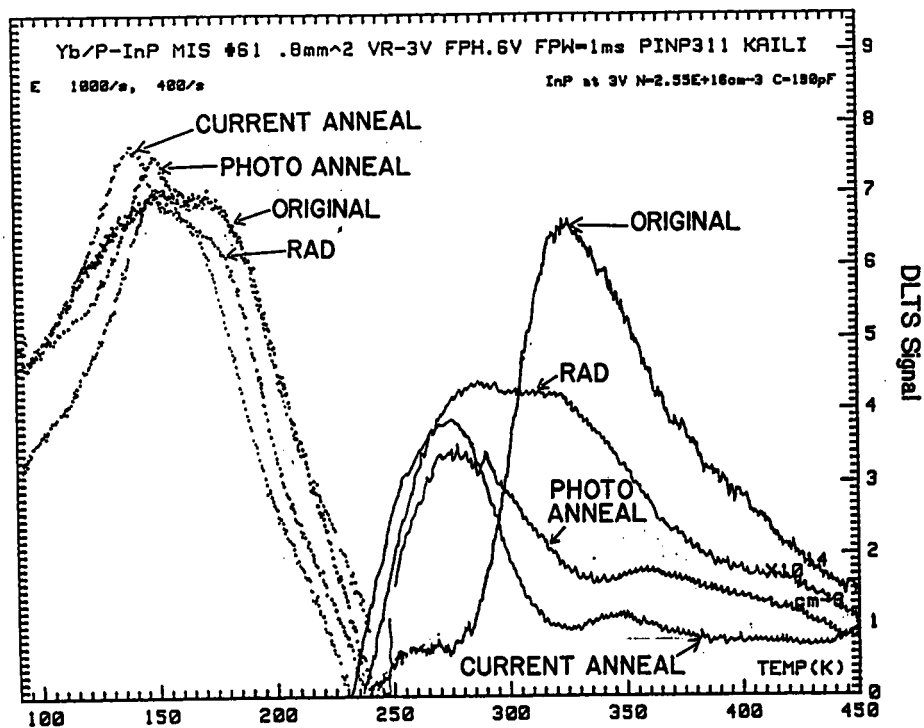


Figure 6 Series of DLTS scans showing different stages of irradiation and annealing for a Yb-MIS diode.